

## Mineralogy and Genesis of Manganese Ores from the Jangseong Manganese Deposits, Korea

Soo Jin Kim\* and Hyeon Yoon\*

**Abstract:** The Jangseong manganese deposits are supergene oxidation products of hydrothermal rhodochrosite. The manganese ore veins are developed in the Dongjeom Quartzite, and Dumudong Formation. The deposits consist of primary manganese carbonate ores in the deeper part and manganese oxide ores near the surface. The manganese carbonate ores are composed of rhodochrosite and small amounts of sulfides. The manganese oxide ores are composed of birnessite, nsutite, todorokite, chalcophanite, and pyrolusite. Microscopic, X-ray diffraction, infrared, thermal and EPMA analyses have been made for manganese oxide minerals and other associated minerals.

The manganese minerals were formed in the following sequence.

Rhodochrosite→birnessite→todorokite→nsutite→pyrolusite.

Thermochemical properties of chalcophanite were studied by methods of X-ray powder diffraction, infrared absorption spectroscopic analysis and dehydration experiments. Chalcophanite changes to 4.8Å phase at 90~110°C. Chemical analyses show that the manganese oxide minerals generally have high concentration in Zn.

### INTRODUCTION

#### General Statement

The Jangseong manganese deposits are located in Jangseongdong, Taebag-si, Gangweon-do (Lat. 37°06'15"–37°07'05", Long. 129°00'–129°02), Korea.

The outcrop of the ore vein is found on the slope of mountain about 1.6 Km south of Jangseong.

One short tunnel has been opened for prospecting without production of any commercial ores.

The deposits consist of manganese oxide ores near the surface and manganese carbonate-sulfide ores in depth. Recently, the Yeongpung mining Co. drilled the area in order to know the nature of mineralization of the vein in depth. From this drilling, they could confirm that the sulfide-carbonate mineralization continues to a considerable

depth and finally changes to a large sulfide ore body.

This work aims at the study of the mineralogy and genesis of manganese ores from the Jangseong manganese deposits.

#### Procedures and Methods of Study

This work was made by methods of field investigation and laboratory works. Various types of ores were sampled systematically for the laboratory works. Laboratory works were made by the following methods.

Observation under the microscope: All the samples were studied under the stereomicroscope. Samples for the preparation of polished sections were also selected under the stereomicroscope.

Polarizing and ore microscopic observation: Total 90 polished sections and 20 thin sections were prepared and studied under the microscope. In order to prepare polished sections, samples cut with diamond saw were impregnated in polyester in vacuum jar for five minutes or more. After the perfect hardening of polyester,

\*Department of Geological Sciences, Seoul National University, Seoul 151, Korea

they were carefully ground and polished with  $5\mu$  alumina,  $1\mu$  diamond pastes, and  $0.03\mu$  alumina successively.

All the polished sections were studied under the microscope to know the optical properties, textures, and paragenetic position of each mineral.

X-ray powder diffraction analysis: A JEOL model JDX-5P diffractometer, and Debye-Scherrer camera of diameter of 114.6 mm were used for the identification and structural characterization of each mineral in the manganese ores.

Infrared absorption spectroscopic analysis: Infrared absorption spectroscopic analysis was made to know the spectroscopic characters of the manganese oxide and other minerals.

Perkin-Elmer model 283B spectrophotometer was used on the KBr pellets for the 4000 to  $200\text{ cm}^{-1}$  region. Approximately 3 mg of powdered sample dispersed in KBr was pressed for 5 min. at 1.2 kbar under vacuum. Conditions of spectrophotometer were scan time 6 minutes, slit program 6, expansion 1. The spectra were calibrated with polystyrene film.

Thermal analysis: Thermal analysis was made

for chalcophanite and todorokite. DTA, TG and DTG curves were obtained simultaneously with a Rigaku Thermoflex and a model PTC-10A temperature controller.

Conditions for thermal analysis are as follows:

Atmosphere : air

Reference :  $\text{Al}_2\text{O}_3$

DTA :  $\pm 50\mu\text{V}$

DTG : 2 mg/min.

TG : 10 mg full scale

Heating rate :  $10^\circ\text{C}/\text{min}$ .

Chart speed : 5 mm/min.

Dehydration experiment: Dehydration experiments of chalcophanite were made by Hitachi model IRC-2 temperature controller and digital thermocouple. Heat-treated samples were studied by the X-ray powder diffraction and the infrared absorption spectral analysis.

Electron probe microanalysis: Quantitative chemical analyses were made using the electron probe microanalyzer in the Institute for Mineralogy, Heidelberg University.

Eight elements including K, Zn, Ca, Mg, Fe, Na, and Mn were quantitatively determined.

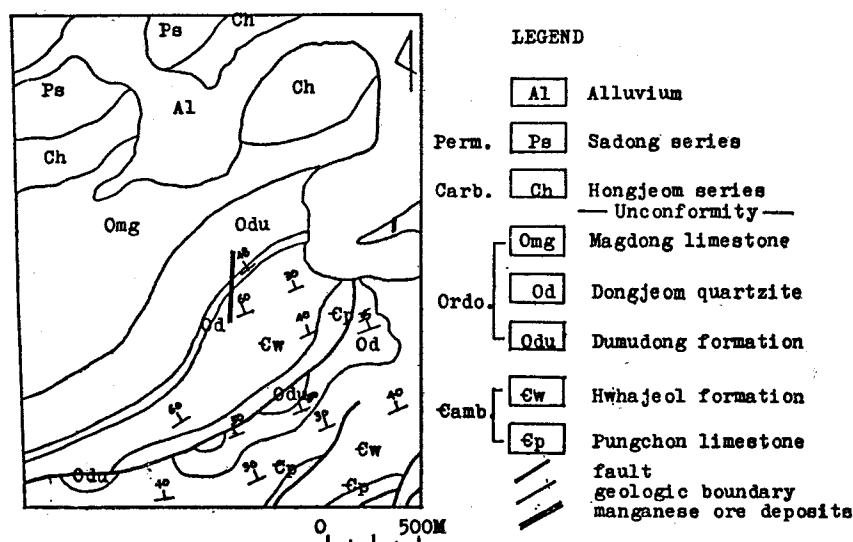


Fig. 1 Geologic map of the Jangseong manganese deposits.

## GENERAL GEOLOGY

The geology around the Jangseong manganese deposits consists of the Pungchon Limestone, and Hwajeol Formation of Cambrian age, and Dongjeom Quartzite, Dumudong Formation, and Magdong Limestone of Ordovician age in the ascending order (Fig. 1).

The geological sequence of the rocks in the area of Jangseong manganese deposits is as follows:

Ordovician	{	Magdong Limestone
		Dumudong Formation
		Dongjeom Quartzite
Cambrian	{	Hwajeol Formation
		Pungchon Limestone

Manganese ore veins are developed crossing the Dongjeom Quartzite and the Dumudong Formation. They show the strike of N5-10°E and the dip of 75-80°SE. The width of the main vein is about 80-100 cm. Several thin veins are also developed parallel to the main vein.

## MANGANESE ORE DEPOSITS

Manganese ore deposits at Jangseong are genetically grouped into two types: hypogene and supergene deposits. Hypogene manganese ores are composed of manganese carbonate with minor sulfides, and supergene manganese ores of manganese oxides.

Manganese carbonate ores are generally not found near the surface, but below the manganese oxide ore bodies.

Manganese oxide ore deposits are developed near the surface. The main manganese oxide ore vein is 1 m or less in width. It shows the strike of N 5-10°E and the dip of 75-80°SE.

## MANGANESE ORES

### Manganese and Associated Minerals

Manganese ores are composed of manganese carbonate and oxide minerals.

Manganese carbonate ores consists chiefly of rhodochrosite and sulfides such as sphalerite, arsenopyrite, chalcopyrite, galena, and pyrite.

The manganese oxide ores were formed from the hypogene manganese carbonate minerals by supergene oxidation by the action of ground water and oxygen under the surface condition.

Manganese oxides consists of birnessite, chalcofanite, nsutite, pyrolusite, and todorokite.

### Types of Ores

According to the megascopic observation on the manganese oxide ores, there are two major types of manganese oxide ores: a) ores formed by replacement, and b) ores formed by precipitation.

Ores formed by replacement: Most of manganese oxide minerals were formed by replacement, which includes the oxidation of primary manganese carbonate ores, further oxidation of early-formed oxide phases, and the substitution of other minerals by manganese oxides.

The manganese oxide ores formed by replacement from rhodochrosite show rhombic or leaf-like pseudomorphs of manganese oxides after rhodochrosite. They are generally fine-grained and compact.

Ores formed by precipitation: This type of ore shows colloform bands, spherulitic or sub-parallel aggregates, cavity-filling and -lining textures. The manganese oxides of this type have been formed by colloidal and/or non-colloidal precipitation.

## MINERALOGY OF MANGANESE AND ASSOCIATED MINERALS

### General Statement

Naturally occurring manganese oxides usually occur as fine-grained mixture of two or more kinds of minerals. Preparation of pure samples was only possible by taking them with sharp knife under the microscope with high magnification. Identification of mineral species is usually

made by X-ray diffraction. However, it is difficult and sometimes impossible because of poor crystallinity. X-ray powder diffraction lines are frequently broad and diffuse.

Infrared spectroscopy is generally accepted as useful supplement to X-ray diffraction for identification of manganese oxide minerals, because it is sensitive to low crystalline to amorphous compounds. But it is not a primary structural technique like X-ray diffraction.

**Manganese Oxide Minerals**

**Birnessite**

Occurrence: Birnessite in the Jangseong manganese deposits occurs as two types: birnessite pseudomorphous after rhodochrosite with distinct rhombic cleavages (Figs. 8 and 9) and birnessite formed by precipitation or open space-filling (Fig. 10).

Birnessite pseudomorphous after rhodochrosite is nearly isotropic to cryptocrystalline. In case, it is associated with dendritic todorokite.

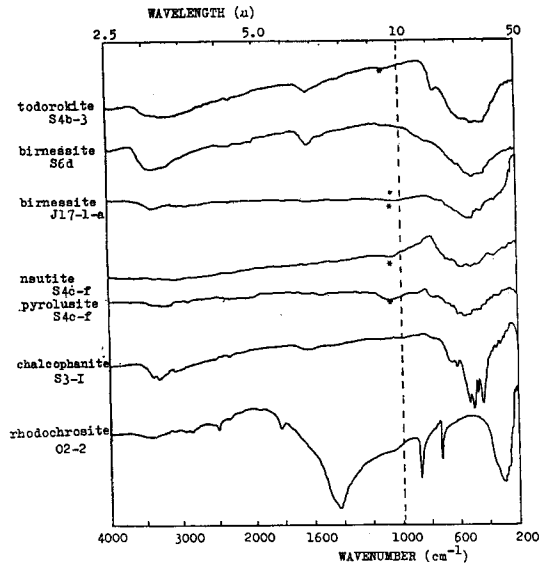


Fig. 2 Infrared absorption spectra for manganese minerals from Jangseong manganese ore deposits.

\* absorption bands due to quartz impurity

Physical and optical properties: Birnessite is grayish black to dark purple gray in colour, dark

Table 1 X-ray powder diffraction data of manganese oxide minerals from Jangseong manganese deposits (FeK $\alpha$ /Mn).

todorokite (S4b-3)			birnessite (S1-1c)			nsutite (S4c-f)			pyrolusite (S4c-f)			chalcophanite		
I	d(Å)	hkl	I	d(Å)	hkl	I	d(Å)	hkl	I	d(Å)	hkl	I	d(Å)	hkl
s	9.63	001	sb	7.05		sb	3.980	101	vs	3.117	110	s	6.938	100
s	4.807	002	w	3.552		w	2.604	211	s	2.406	101	w	6.158	010, $\bar{1}01$
w	3.351	003	s	2.442		s	2.438	200	m	2.107	111	s	4.054	011, $\bar{1}\bar{1}1$
w	2.461	012	s	2.389		m	2.344	301	vw	1.987	210	s	3.482	$\bar{1}12, 002$
w	2.298	004	vw	2.154		s	2.137	221	sb	1.626	211	w	3.356	121, 221, $02\bar{1}$
w	1.428	020	w	1.423		w	2.078	311	m	1.562	220	m	2.763	$\bar{2}22, 022, 012$
						sb	1.649	222	m	1.437	002	m	2.553	021, $\bar{1}22$
						w	1.416	600	w	1.304	301	m	2.451	$\bar{1}13, 231$
						m	1.370	340	w	1.057	222	m	2.403	$\bar{1}13, \bar{2}31$
												s	2.232	$\bar{1}31, 21\bar{3}$
												m	2.125	$\bar{2}32, 12\bar{3}$
												w	1.975	013
												m	1.929	$\bar{1}32$
												w	1.847	$\bar{3}33, 031$
												m	1.794	$\bar{3}41, \bar{2}33$
												w	1.661	
												s	1.596	
												w	1.562	

**Table 2** Infrared absorption bands of manganese oxide minerals from the Jangseong manganese deposits.

birnessite		birnessite		todorokite		chalcophanite		nsutite		pyrolusite	
cm <sup>-1</sup>	I	cm <sup>-1</sup>	I	cm <sup>-1</sup>	I	cm <sup>-1</sup>	I	cm <sup>-1</sup>	I	cm <sup>-1</sup>	I
265	w	265	w	285	w			265	w		
						315	w			320	w
350	w	350	w	350	w	345	m	360	w		
415	m	440	m	420	s	440	vs			410	w
		470	w			472	s	465	m		
500	vs	500	vs	500	s	500	s				
540	m	530	s	565	w	530	s	522	s	535	s
								578	s	565	s
						615	m			610	s
		670	w			650	m	650	w		
				760	m			680	w	685	w
										795	w
1,625	w	1,635	w	1,635	m	1,635	w				
3,400	s	3,400	s	3,280	s	3,325	s	3,400	w		
						3,420	s				

brown in streak, earthy in luster and show low to moderate hardness.

Under the ore microscope, it is gray to brown in colour, nearly isotropic and shows no internal reflection.

X-ray powder diffraction data: X-ray powder diffraction data of birnessite are given in Table 1.

Infrared absorption spectrum: The infrared absorption spectra of birnessite from Jangseong manganese deposits are shown in Fig. 2, and the absorption bands are given in Table 2.

Chemistry: The quantitative chemical analyses of birnessite were carried out using the electron probe microanalyser. Their results are given in Table 3. It is characteristic of birnessite from the Jangseong deposits that it contains high Zn.

#### Nsutite

Occurrence: Nsutite occurs as a major constituent of manganese oxide ores. It shows colloform bands with birnessite (Fig. 10) or todorokite. It replaces todorokite (Figs. 11 and 14). Massive botryoidal nsutite is hard and microcrystalline. It also shows shrinkage cracks (Fig.

**Table 3** Electron probe microanalyses for birnessite, todorokite, chalcophanite, and nsutite.

	birnessite	chalcophanite	todorokite	nsutite	
K <sub>2</sub> O	1.60	0.08	0.46	0.48	0.41
ZnO	4.12	13.18	8.04	2.48	1.97
CaO	2.32	0.80	1.61	1.11	0.65
MgO	0.56	0.09	0.20	0.11	0.07
TiO <sub>2</sub>	0.06	0.00	0.00	0.00	0.01
FeO	0.00	0.00	0.00	1.79	6.33
Na <sub>2</sub> O	0.12	0.00	0.00	0.04	0.05
MnO	66.66	57.75	61.67	69.69	68.06
total	75.44	71.90	71.98	75.70	77.55

14). Nsutite formed by direct precipitation from solutions does not show shrinkage cracks (Zwickler et al., 1962; Kim, 1975).

Physical and optical properties: Nsutite is dark grayish black in colour, black in streak, metallic in luster, and very hard (H=8).

In the reflected light, it shows pale creamy white colour and very high reflectance, distinct bireflectance.

X-ray powder diffraction data: X-ray powder diffraction data of nsutite are given in Table 1.

Infrared absorption spectrum: Infrared absorption spectrum of nsutite is shown in Fig. 2 and absorption bands are given in Table 2.

Chemistry: The quantitative chemical analysis of nsutite was carried out using the electron microprobe, and the result is given in Table 3. It is remarkable that nsutite contains considerable amount of Zn.

#### Todorokite

Occurrence: Todorokite is found as a major manganese oxide phase in the Jangseong manganese deposit. It occurs as three types; a) massive todorokite replacing the manganese carbonate ores or early formed manganese oxide mineral (Fig. 14), b) spherulitic and subparallel aggregates (Fig. 12), and c) frost-like acicular todorokite (Fig. 13) forming dendritic aggregates.

Spherulitic todorokite is nearly pure, and well-crystallized as evidenced by X-ray powder diffraction. It is associated with birnessite, chalcophanite, and pyrolusite. Last two types of todorokite might have been formed by precipitation from solution.

Physical and optical properties: Todorokite is brownish black in colour, dark brown in streak, and submetallic to earthy in luster. Hardness is lower than chalcophanite and nsutite. In the reflected light, it shows greenish yellow to pale yellow colour, strong anisotropism, undulatory extinction, and no internal reflection. But in the poorly polished sections, it shows strong internal reflection similar to rancieite.

X-ray powder diffraction data: X-ray powder diffraction data of todorokite are given in Table 1. The X-ray diffraction patterns were indexed on an orthorhombic unit cell with  $a=9.618$ ,  $b=2.849$ ,  $c=9.590$  Å. The axial ratio  $a:b:c=3.376:1:3.366$ . They have been refined by the lattice constant Least-Squares Refinement Program, LCLSQ (MIV) (Burnham, 1970). No systematic correction term has been used.

Infrared absorption spectrum: Infrared absorp-

tion spectrum of todorokite is shown in Fig. 2. Positions of absorption bands are given in Table 2.

Chemistry: Quantitative chemical analyses of todorokite was performed using electron probe microanalyser, and the result is given in Table 3. It is remarkable that todorokite contains a considerable amount of Zn.

Thermal behavior: DTA, TG, and DTG curves for todorokite are shown in Fig. 3. DTA curve shows four endothermic peaks at 47°C, 107°C, 143°C and 635°C. The first three represent loss of water. The peak at 47°C is due to the loss of absorption water, those at 107°C and 143°C, probably due to the loss of crystallization water. Strong endothermic peak at 625°C is due to the loss of oxygen, resulting in the phase transformation to  $Mn_2O_3$ .

#### Chalcophanite

Occurrence: Chalcophanite occurs as spherulitic (Fig. 15) or tabular (Fig. 16) crystals in association with goethite.

Tabular crystals of chalcophanite has twin-like intergrowths and oriented roughly parallel to (001). Chalcophanite has a basal cleavage. It is observed that chalcophanite replaces todorokite.

Physical and optical properties: Chalcophanite is dark gray in colour, dark brown in streak and metallic in luster. It has relatively higher hardness than todorokite.

In the reflected light, it shows creamy white colour, strong birefractance, and strong aniso-

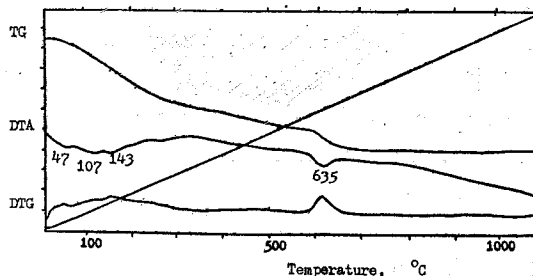


Fig. 3 Thermal curves for todorokite.

tropism.

X-ray powder diffraction data: X-ray powder diffraction data of chalcophanite are given in Table 1. The X-ray diffraction patterns are indexed on a triclinic unit cell with parameter  $a=7.94$ ,  $b=7.71$ ,  $c=8.58 \text{ \AA}$ ,  $\alpha=86.37^\circ$ ,  $\beta=120.89^\circ$ ,  $\gamma=122.38^\circ$ . The axial ratio is  $a:b:c=1.029:1:1.112$ . They have been refined by the lattice constant Least-Squares Refinement Program, LCLSQ(MIV) (Burnham, 1990).

Infrared absorption spectrum: Infrared absorption spectrum of chalcophanite is shown in Fig. 2, and absorption bands are given in Table 2.

Chemistry: The quantitative chemical analysis of chalcophanite was carried out using the electron probe microanalyzer, and the results are given in Table 3.

Thermal behavior: DTA, TG and DTG curves of chalcophanite are shown in Fig. 4. X-ray diffraction patterns of heat-treated sample for 15 minutes at each temperature are shown in Fig. 5.

Endothermic peak at  $45^\circ\text{C}$  is due to the loss of adsorption water. Peak  $156^\circ\text{C}$  is probably due to the loss of interlayer water in chalcophanite structure and the transformation to a new  $4.8 \text{ \AA}$  phase with characteristic  $4.8$  and  $2.4 \text{ \AA}$  peaks. Heating experiment (Fig. 5) shows that the transformation took place at about  $90\text{--}110^\circ\text{C}$ .

The infrared absorption spectra taken for heat-treated chalcophanite are shown in Fig. 6. The spectrum of room temperature shows two distinct absorption bands at  $3325$  and  $3420 \text{ cm}^{-1}$  wave-

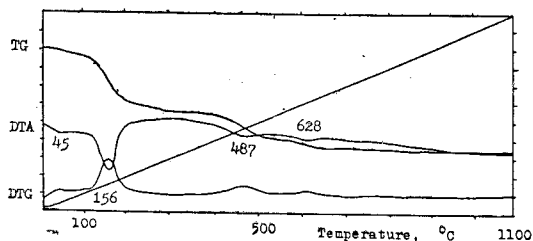


Fig. 4 Thermal curves for chalcophanite.

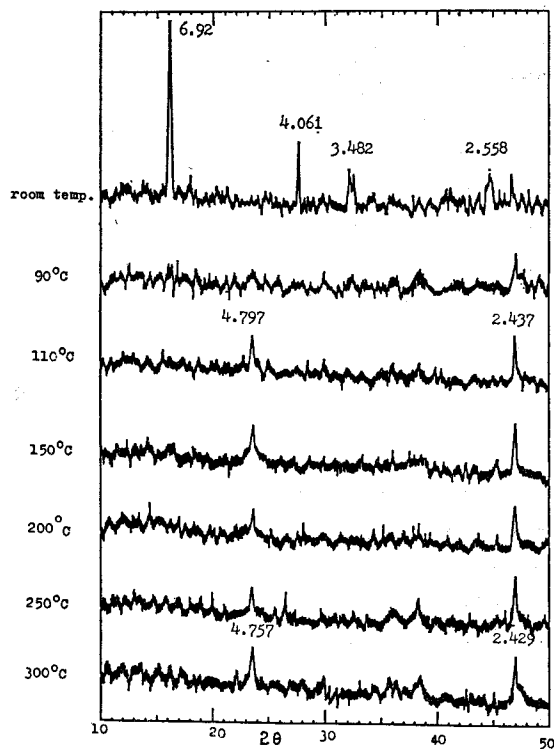


Fig. 5 X-ray powder diffraction patterns for chalcophanite heated.

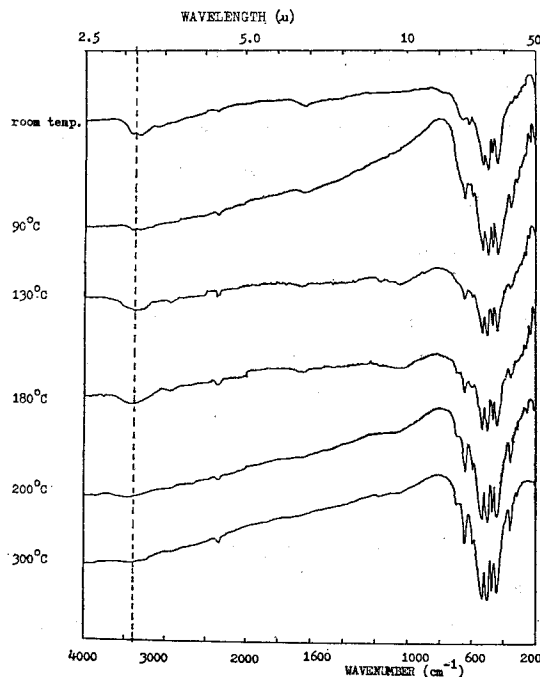


Fig. 6 Infrared absorption spectra for heat-treated chalcophanite.

number. In the chalcophanite structure, all water molecules are structurally equivalent, showing weak hydrogen-bonding between water molecules (Potter, 1979).

#### **Pyrolusite**

Occurrence: Pyrolusite occurs as two distinct types: a) radiating aggregates or columnar crystals (Fig. 18) along the walls of nsutite in cavities, b) massive pyrolusite (Fig. 17).

In some cases, it replaces colloform birnessite. It is associated with todorokite, nsutite, and chalcophanite.

Physical and optical properties: Pyrolusite is iron black in colour, and black to dark gray in streak, and metallic in luster. Hardness is moderate to hard.

Under the reflected light, it shows yellowish white or creamy yellow colour, strong birefractance, strong anisotropism, and no internal reflection.

X-ray powder diffraction data: X-ray powder diffraction data of pyrolusite are given in Table 1.

Infrared absorption spectrum: Infrared absorption spectrum of pyrolusite is shown in Fig. 2, and absorption bands are given in Table 2.

### **Manganese Carbonate and Associated Minerals**

#### **Rhodochrosite**

Rhodochrosite is usually pink in colour but in case pinkish gray due to impurities. It generally shows large rhombohedral crystals in geodes or veinlets. It is oxidized to manganese oxides near the surface.

Pink gray to pink coloured rhodochrosite has moderate hardness, and vitreous luster.

Under the polarizing microscope, it is colourless to pale pinkish brown, and shows strong pleochroism and strong internal reflection in polished sections.

#### **Goethite**

Goethite is found in most of the manganese

oxide ores. It is frequently associated with todorokite and birnessite in cavities. It occurs as pseudomorph after pyrite in manganese oxide ores. It forms contact rims around chalcophanite.

#### **Sulfides**

The sulfide minerals found in manganese ores are arsenopyrite, chalcopyrite, galena, pyrite, and sphalerite. These sulfide minerals are associated with manganese carbonate ores, and replaced by goethite.

#### **Quartz**

Quartz is the most frequent gangue mineral in manganese ores. It shows euhedral to anhedral crystals.

## **TEXTURES AND STRUCTURES OF ORES**

### **Primary Oxidation Textures**

One of the abundant supergene primary textures of the manganese oxide ores are replacement texture which has been formed by oxidation of hypogene rhodochrosite (Figs. 8 and 9). The relict fabrics of rhombic rhodochrosite are abundantly found in the manganese oxide ores in contact with rhodochrosite.

This type of texture is usually found in the birnessite ores.

### **Precipitation Textures**

Precipitation from colloidal or noncolloidal solution in the open space of manganese oxide ores produced precipitation textures such as colloform (Fig. 10), cavity-filling, and -lining (Figs. 16 and 18).

Minerals showing these textures are birnessite, todorokite, and nsutite.

### **Replacement Textures**

Replacement textures are resulted from the oxidation of rhodochrosite and the further oxidation of early formed manganese oxides and the replacement of other minerals by manganese oxide phases.

Replacement textures of birnessite by todorokite, of todorokite by nsutite (Figs. 11 and 14)



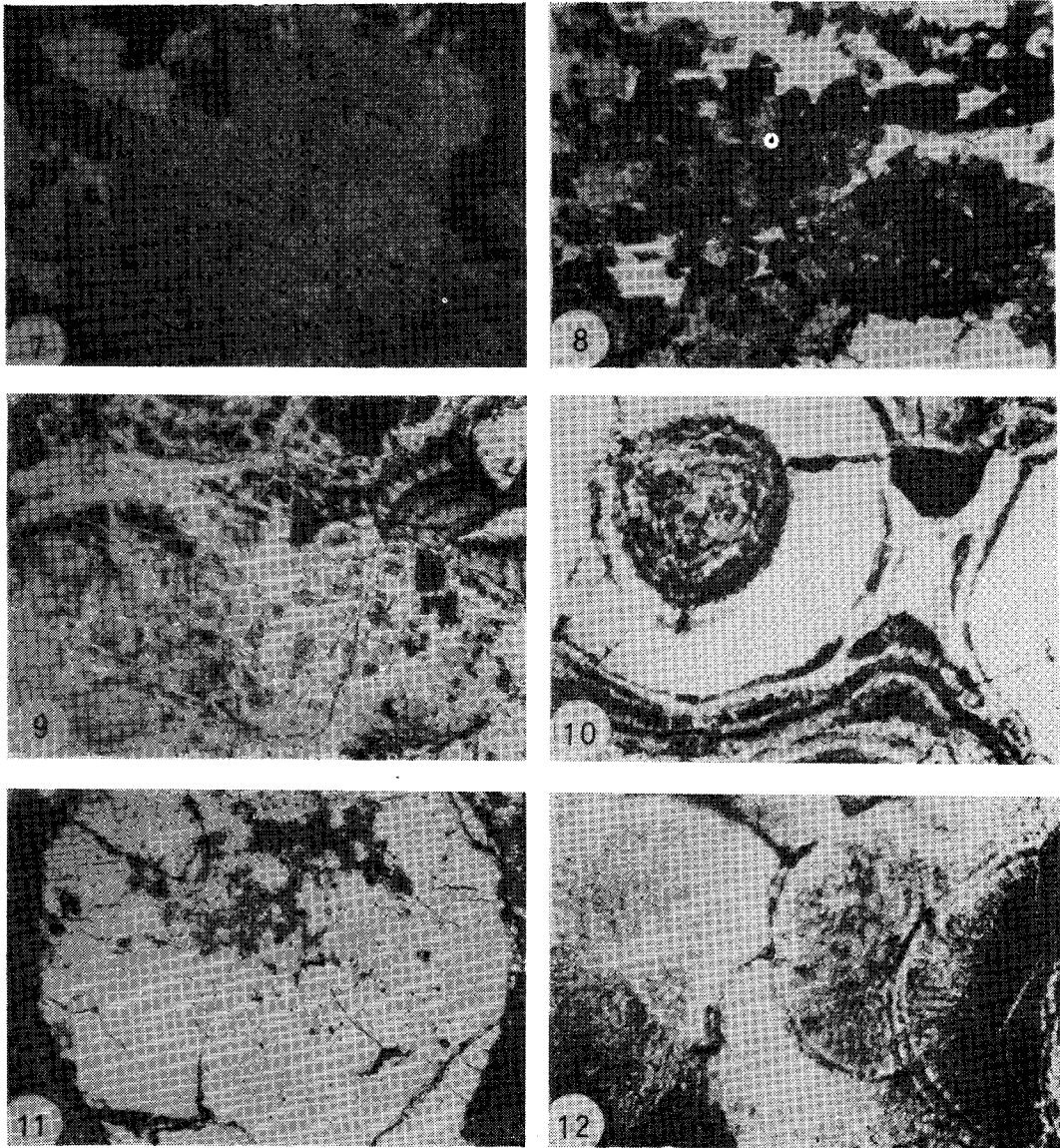


**Fig. 7** Rhodochrosite showing distinct rhombic cleavage and growth zoning.  $\times 40$ . Nicols crossed. Thin section.

**Fig. 8** Rhodochrosite (grey) is partly oxidized to manganese oxides (black).  $\times 40$ . Nicols crossed. Thin section.

**Fig. 9** Birnessite having relict rhombic cleavage of rhodochrosite.  $\times 60$ . Polished section. Nicols not crossed.

**Fig. 10** Colloform nsutite (white) and birnessite (grey).  $\times 100$ . Polished section. Nicols not crossed.

**Fig. 11** Todorokite (grey) replaced by nsutite (white).  $\times 100$ . Polished section. Nicols not crossed.

**Fig. 12** Spherulitic todorokite.  $\times 100$ . Polished section. Nicols crossed.

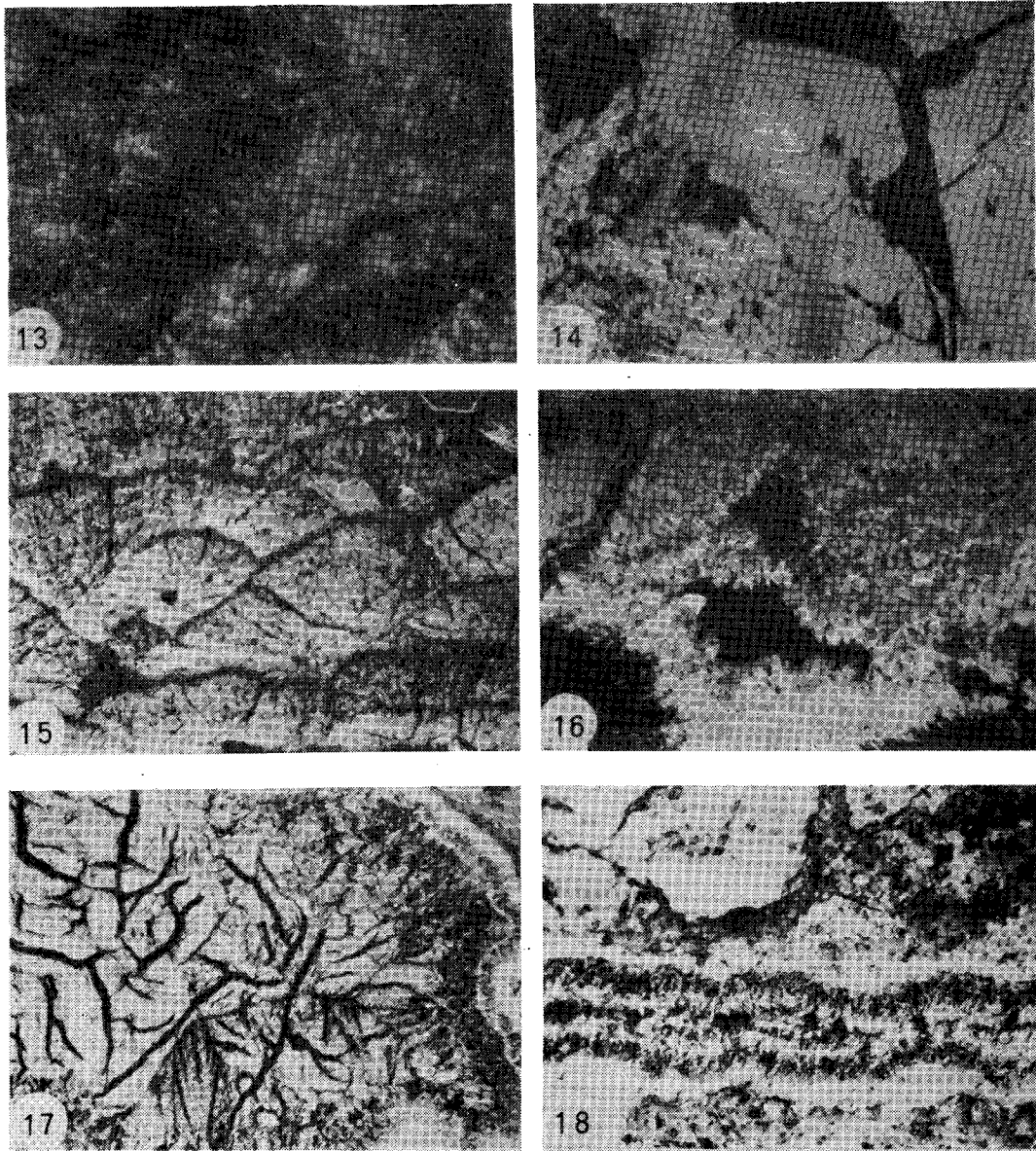


**Fig. 13** Fibrous todorokite.  $\times 100$ . Polished section. Nicols crossed.

**Fig. 14** Pyrolusite (grey) crossing todorokite (light grey in left) and nsutite (white in right). Todorokite is replaced by nsutite.  $\times 100$ . Polished section. Nicols not crossed.

**Fig. 15** Fan-like chalcophanite.  $\times 100$ . Polished section. Nicols not crossed.

**Fig. 16** Chalcophanite crystal aggregates.  $\times 100$ . Polished section. Nicols not crossed.

**Fig. 17** Shrinkage cracks in pyrolusite.  $\times 100$ . Polished section. Nicols not crossed.

**Fig. 18** Tiny pyrolusite crystals along the wall of crack in nsutite.  $\times 100$ . Polished section. Nicols not crossed.

or pyrolusite (Fig. 14), and of nsutite by pyrolusite (Fig. 14) are observed.

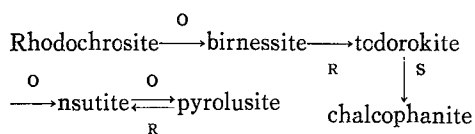
**GENESIS OF MANGANESE ORE DEPOSITS**

Field occurrence of manganese ores and their textures in the Jangseong manganese deposits indicate that the manganese oxide ores were formed from the manganese carbonate ores by the supergene processes.

The oxidation of the manganese carbonates took place along the cleavages, grain boundaries, and fractures, and proceeded outward, forming more manganese oxide minerals.

Some ores might have been formed by filling of the colloidal or non-colloidal solutions in cavities.

The textural study of the manganese ores from the Jangseong manganese deposits shows that the manganese minerals were formed from the protore minerals in the following sequence.



(o: oxidation, r: reduction, s: simple sequence)

**SUMMARY AND CONCLUSIONS**

The conclusions reached from the study on the mineralogy, textures, structures, chemistry, and genesis of the manganese oxide ores in the Jangseong manganese deposits are summarized in the following.

1) The geology of the Jangseong manganese deposits consists of the Pungchon Limestone, and Hwajeol Formation of Cambrian age, Dongjeom Quartzite, Dumudong Formation, and Magdong Limestone of Ordovician age. The manganese ore vein shows the strike of N 5-10°E and the dip of 75-80°SE.

2) The manganese oxide ore deposits have been formed by supergene oxidation of hydro-

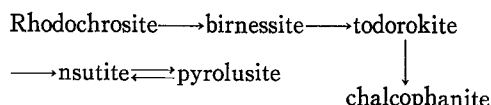
thermal rhodochrosite-sulfide vein.

3) The manganese oxide ores are composed of birnessite, chalcophanite, nsutite, todorokite, and pyrolusite, with other minerals such as goethite, quartz, and sulfides.

4) Dehydration experiments of chalcophanite shows that it transforms to a new 4.8 Å phase at about 90-110°C

5) The chemical analyses show that the manganese oxide minerals from the Jangseong manganese deposits generally has high concentration in Zn.

6) The manganese oxide ores were formed by oxidation, replacement, and precipitation from solution. The trend of formation of manganese oxides is as follows:



**ACKNOWLEDGMENT**

The present study was supported financially by the Basic Science Research Institute Program of the Ministry of Education in 1984. Sincere thanks are extended to the Ministry of Education for the financial support.

**REFERENCES**

Kim, S.J. (1979) The stratabound manganese carbonate deposits of the Janggun mine, Korea. Mineral Deposits, Monograph No. 18, 79p, Stuttgart.

Kim, S.J. (1980) Birnessite and rancieite problem: their crystal chemistry and new classification. J. Geol. Soc. Korea, v. 16, p. 105-113.

Potter, R.M. and Rossman, G.R. (1979) The tetravalent manganese oxides: identification, hydration and structural relationships by infrared spectroscopy. Amer. Mineral., v. 64, p. 1199-1218.

Wadsley, A.D. (1955) The crystal structure of chalcophanite, ZnMn<sub>3</sub>O<sub>7</sub>·3H<sub>2</sub>O. Acta crystal., v. 8, p. 165-172.

Zwicker, W.K., Groeneveld Meijer, W.O.J. and Jaffe, H.W. (1962) Nsutite, a widespread manganese

## 長省 망간 鑛石에 對한 鑛物學的 및 成因의 研究

金 洙 鎮 · 尹 惠 溫

**요약** : 장성망간광상은 주로 두무동층과 동점규암층을 횡단하는 맥상광체로 산출된다. 본 지역의 망간광맥은 대체로 N5-10°E의 주향과 75-80°SE의 경사를 보인다.

망간광체는 일차적으로 열수기원의 탄산망간광석과 이의 표성산화물인 산화망간광석으로 구성되어 있다. 탄산망간광석은 주로 능망간석으로 구성되어 있고 약간의 황화광물들을 수반한다. 산화망간광석은 비어네사이트·켈코파나이트, 토도로카이트, 엔소타이트, 연망간석으로 구성되어 있다. 탄산망간광물은 다음과 같은 순서로 산화되어 산화망간광물들이 형성되었다.

능망간석 → 비어네사이트 → 토도로카이트 → 엔소타이트 ⇌ 연망간석

한편 토도로카이트와 켈코파나이트는 후기에 공동에서 침전에 의하여 형성되기도 했다.

켈코파나이트의 열화학적 성질을 X선회절분석, 적외선흡수분광분석, 열분석, 전자현미분석, 가열실험 등에 의하여 연구한 결과 90~110°C에서 4.8Å상으로 상변화하였다.

비어네사이트, 토도로카이트, 엔소타이트, 켈코파나이트 등의 전자현미분석 결과 본 광상에서 산출되는 산화망간 광물들은 대체로 Zn을 비교적 많이 함유하고 있음이 밝혀졌다.

